Sulfidized Fe-C nanocomposite powders produced by one-step laser pyrolysis technique

C. FLEACA[a,b,*], I. MORJAN[a], F. DUMITRACHE[a], A.-M. NICULESCU[a], A. BADOI[a], C. LUCULESCU[a], E. VASILE[c], G. PRODAN[d], L. VEKAS[e]

[a]*National Institute for Lasers. Plasma and Radiation Physics NILPRP, 409 Atomistilor str., Magurele, Bucharest, Romania*

[b]*"Politehnica" University of Bucharest, Physics Department, 313 Independentei blv., Bucharest, Romania*

[c]*"Politehnica" University of Bucharest, Faculty of Applied Chemistry and Materials Science, Science and Engineering of Oxide Materials and Nanomaterials Department, 1-7 Gh. Polizu str., Bucharest, Romania*

[d]*"Ovidius" University of Constanta, 124 Mamaia blv., Constanta, Romania*

[e]*Romanian Academy, Timisoara Branch, 24 Mihai Viteazul blv., Timisoara, Romania*

Laser pyrolysis was employed to synthesize iron-based magnetic nanocomposites from fixed $Fe(CO)_5$ and various CS_2 vapor flows by using C_2H_4 as sensitizer. The resulted nanopowders were composed from a mixture of iron-containing phases: metallic, carbides, oxide (maghemite) and sulfide (pyrrhotite). The γFe_2O_3 was formed after post-synthesis air exposure, the highest oxygen content being found in the powder obtained from the lowest CS_2 flow. TEM images reveal aggregates of core-shell nanoparticles (7-25 nm in size) for the sample with the highest sulfur content, whereas chained particles (15-30 nm) with empty core/porous shell morphology was observed for those with the lowest sulfur content.

(Received June 10, 2014; accepted June 24, 2015)

Keywords: Fe-based core-shell nanocomposites, Pyrrhotite, Laser pyrolysis, Magnetism

1. Introduction

Fe-based nanoscale particles can contain iron in various forms: either metallic or carbidic as Fe^0 (zerovalent) or ionic as Fe^{2+} and/or Fe^{3+} or even as mixtures of them. The zerovalent metallic Fe nanoparticles (usually stabilized with a thin oxide layer) have been used for water purification by the degradation of organic contaminants (especially halogenated compounds) [1], [2] or precipitation/sequestration of toxic inorganic ions such as Cr(VI) or Pb(II) [3]. The most utilized and studied ionic iron-containing nanoparticles are the oxides Fe_3O_4 (magnetite) and Fe_2O_3 (gamma phase - maghemite or alpha phase - hematite). The first two phases have a relative high magnetization (with ferrimagnetic or superparamagetic behavior), whereas the last is a weak magnet (antiferromagnetic). Due to their biocompatibility associated with good magnetic properties and the possibility to be coupled with various functionalized molecules, the Fe_3O_4 or γFe_2O_3 nanoparticles have wide applications in biomedicine for diagnosis (as MRI contrast agents [4] or fluorescent markers [5]) and therapy (as drug carriers [6] or hyperthermia agents [7]). Much less reported, the nanoscale iron sulfides were also used in various applications such as: water treatment (aqueous dechlorination of C_2Cl_4 pollutant (using cobalamin) [8], La(III) absorption (coated with Fe_3O_4) [9], reductive sequestration of radioactive pertechnate $^{99}TcO_4^-$ (starting from Fe^0) [10]), thin film photovoltaics (as colloidal pyrite) [11]), anode material for Li-ion batteries (embedded in carbon microspheres) [12] or catalyst in either solvolysis liquefaction of soda lignin for renewable oil and gas production [13] or coal liquefaction (after sulfidizing of metallic/carbidic nanoiron with $(CH_3)_2S_2$) [14].

The laser pyrolysis is a versatile technique, allowing the continuous manufacturing of various iron-based nanopowders such as carbidic/metallic ones [15] and oxidic (maghemite) [16]. Using the same method, we had also obtained core-shell nanocomposites such as $Fe/Fe_xC@C$ with high [17] or low [18] iron content or $Fe/\gamma Fe_2O_3$@Polycarbosiloxane reticulated polymer [19]. In this paper, we report the use of this method for the synthesis of new metallic/carbidic/sulfidic/oxidic complex multiphase iron-based magnetic nanocomposites.

2. Experimental

As raw materials we used $Fe(CO)_5$ (99.998%) and CS_2 (>99.9%) volatile liquids from Sigma-Aldrich, whereas C_2H_4 (99.95%) sensitizer and auxiliary Ar (99.998%) were purchased from Linde Gas. The experimental set-up was described in [18] and, as presented in the Fig. 1, contains a vertical injector having three concentric nozzles through which the reactive precursors and the ethylene sensitizer (laser energy absorber) are introduced in the reaction chamber where they encounter the focused continuous-wave CO_2 horizontal laser beam (λ = 10.6 μm). Fe and S precursors

are vaporized from separate bubblers using C_2H_4 and Ar, respectively, as carriers and are also separately introduced. The reaction zone (where the nanoparticles are formed) is visible as a small sooting flame protected by an annular Ar coflow. The resulted nanocomposites were entrained by the inert gas and captured next on a porous ceramic filter situated inside the collection chamber, while the gases which passed through pores were directed towards the vacuum pump. The system pressure is kept constant by controlling the incoming and the exhaust flows. The main parameters of the three pyrolysis experiments where we used the same flow of $Fe(CO)_5$ and various CS_2 flows are summarized in the Table 1. The flame temperature was monitored using an IRtec Optical Pyrometer, and the powders atomic composition was obtained using an EDAX device mounted on a SEM FEI Inspect S scanning electron microscope. The nanocomposites morphology was analyzed with a Philips CM120ST transmission electron microscope under 100 kV acceleration voltage, whereas their crystalline phase composition was revealed using a PANalytical X`Pert MPD theta-theta X-ray diffraction (XRD) apparatus using a Cu Kα source (0.15418 nm).

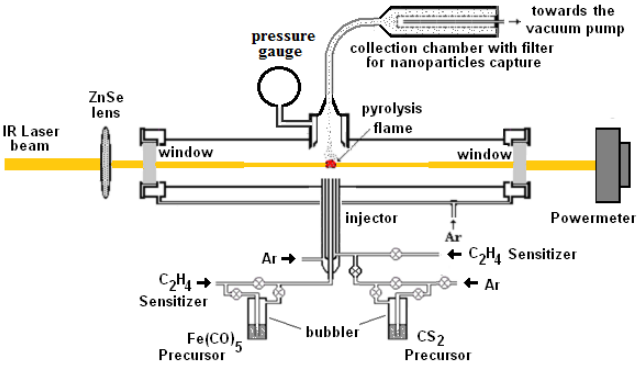

Fig. 1. The experimental set-up for the laser pyrolysis synthesis of the iron-based nanoparticles.

Table 1. The experimental parameters for nanopowders laser pyrolysis synthesis and their atomic composition from EDX analysis.

Sample	Inner flow [sccm]	Second annular flow [sccm]		Laser power density* [W/cm^2]	Flame tem-perature [°C]	EDX elemental composition [atomic %]				
	$C_2H_4/Fe(CO)_5$	Ar/CS_2	C_2H_4			C	O	Fe	S	Fe/S
CF-S1	33/3.33	6.67/3.33	80	3570/3230	~ 638	30.3	24.7	26.8	18.1	1.5
CF-S2	33/3.33	3.33/1.67	80	3400/3170	~ 646	36.1	24.0	26.2	13.7	1.9
CF-S3	33/3.33	1.67/0.83	80	3400/3230	~ 680	33.6	30.0	29.3	11.1	2.6

*****measured without absorption under 100% Ar/ measured after the laser absorption in the reaction zone
Other flows: third annular Ar (2500 sccm) flow for the reactive flows confinement, flushing windows Ar (2 × 750 sccm) flows ; Working pressure: 550 mbar

3. Results and discussions

The simultaneous presence of metallic iron and different iron carbides (Fe_3C cohenite and Fe_7C_3) in the as-synthesized nanopowders (see the diffractogram from Fig. 1) can be explained by the rapid decomposition (sequential decarbonylation) of $Fe(CO)_5$ precursor in the center of the pyrolysis flame under the action of laser-excited ethylene molecules [20]. The resulted $Fe(CO)_{5-x}$ fragments and Fe atoms rapidly coalesce to form hot iron clusters which can act as catalyst for ethylene decomposition and carbon monoxide disproportionation (to carbon and carbon dioxide). The resulted carbon atoms dissolve then into the active iron nanoparticles and, with the temperature reduction after leaving the laser beam, part of them form stoechiometric Fe_3C and Fe_7C_3 carbides and other part precipitates at the particle surfaces, forming a more or less disordered carbonaceous shell. This mechanism is affected by the presence of CS_2 molecules introduced together with Ar and supplementary ethylene on the coflow. The carbon disulfide molecules encounter also hot ethylene molecules, triggering a cascade of chemical reactions. Some of the initial products can be ethylene sulfide and vinylthiol, found also in the silent electrical discharge at atmospheric pressure in CS_2 - C_2H_4 mixture [21]. These molecules can also react to form trithioethylenecarbonate [22] or to further react with other ethylene molecules, forming various sulfur-containing polymers which can undergo dehydrogenation, finally resulting carbon which incorporate sulfur-based groups. Yet, the XRD analyses do not reveal any of elemental sulfur peaks in the obtained nanocomposites. This can be explained by the presence of hydrogen provided by the dehydrogenation reactions, which can react with sulfur to form H_2S. Moreover, the CS_2 hydrogenation reaction can be catalyzed by the transition metal-carbonyl clusters [23]. The resulted hydrogen sulfide can interact with the freshly-formed iron nanoparticles to form iron sulfide. The presence of the sulfide was confirmed by X-ray diffractograms, where the non-stoechiomeric $Fe_{1-x}S$ pyrrhotite phase was identified (see Fig. 2).

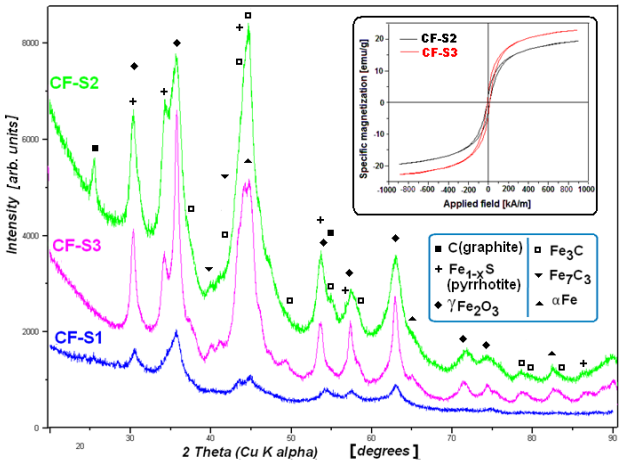

Fig. 2. The superposed X-ray diffractograms of the three nanopowders; right inset: magnetic hysteresis curves of CF-S2 and CF-S3 samples.

From the same figure one can observe that the CF-S1 sample with the highest sulfur content exhibits also the highest disorder degree, reflected by the broad peaks with low intensity. It seems thus that a higher concentration of sulfur compounds in the pyrolysis flame disturbs the nanoparticles crystallization.

Concerning the identification of the maghemite phase in all samples, their presence can only be explained by the post-synthesis reaction with oxygen from the ambient air, since in the pyrolysis processes no reactive oxygen-containing species were introduces. This molecular O_2 partially oxidize the zerovalent iron, similar with the case of the Fe@Fe_2O_3 nanoparticles obtained (also by laser pyrolysis) by us [24]. The highest oxygen content (after EDX measurements) was found in the powder obtained from the lowest CS_2 flow (CF-S3) which also contains the highest amount of iron (see right part of Table 1).

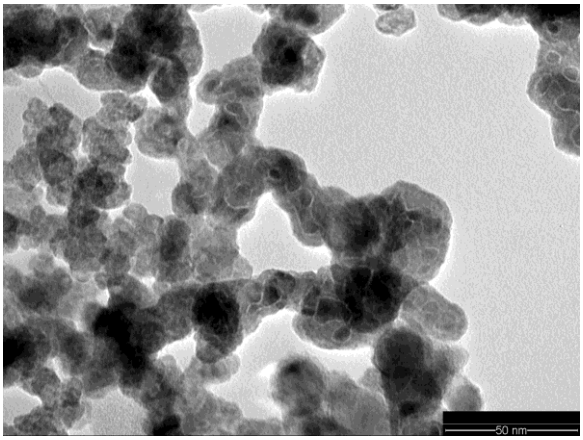

Fig. 3. TEM image from CF-S1 nanopowder.

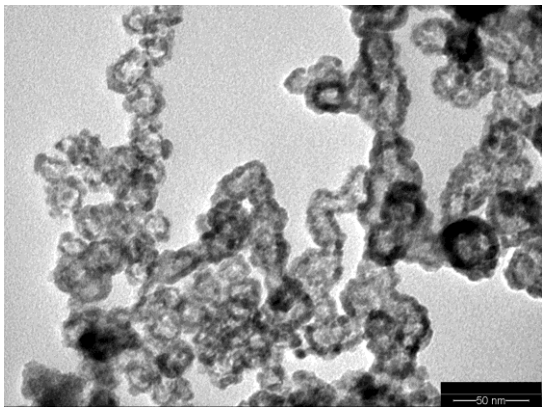

Fig. 4. TEM image from CF-S2 nanopowder.

TEM images of nanopowders from samples CF-S1 (Fig. 3) and CF-S2 (Fig. 4) show different morphologies. For the sample with less crystallinity (CF-S1), aggregated nanoparticles (having sizes between ~ 7 and 25 nm) - many of them with a core-shell morphology - can be observed. In some cases the shells are common to multiple nuclei which seem to be embedded in a less dense conformal matrix. Chained nanostructures are also visible in the TEM image from the more crystalline sample CF-S2, yet their structure consists in porous shells composed from smaller (~ 4 – 6 nm) interconnected nanoparticles which surround an empty core, forming bigger vesicle-like or worm-like nanoparticles with diameters around 15 – 30 nm. These complex morphologies can be a result of the anisotropic oxidation of the metallic/carbidic cores (containing also some sulfide) which are poorly protected by their disordered/discontinuous carbonaceous shells.

Finally, the room temperature hysteresis curves from the more crystalline nanopowders (CF-S2 and CF-S3), presented in the Fig. 2 inset attest their ferro/ferrimagnetic behavior. Their saturation magnetization M_s values (18 emu/g for CF-S2 and 23 emu/g for CF-S3) are near to the ~ 20 emu/g value reported by us for Fe-Fe_2O_3-Polycarbosiloxane core-shell nanoparticles obtained by the same laser pyrolysis method [25]. The higher M_s value of the CF-S3 sample vs. those of CF-S2 powder can be correlated with their higher iron content observed from EDX analysis (see Table 1).

4. Conclusions

In summary, we have synthesized in a single step novel multiphase Fe - S - C - O magnetic nanoparticles using laser pyrolysis technique. The sulfide content can be tuned by controlling the amount of the introduced CS_2 precursor. They can have applications in various fields such as water decontamination/treatment, biomedicine as theranostic agents, liquefaction catalysts for fuel production or anode materials for Li-ion batteries.

Acknowledgements

The work has been funded by the Sectoral Operational Programme Human Resources Development 2007-2013 of the Ministry of European Funds through the Financial Agreement POSDRU/159/1.5/S/132395.

References

[1] T. Raychoudry, T. Scheytt, Water Sci Technol., **68**(7), 1425 (2013).
[2] W. Zhang, J. Nanop. Res **5,** 323 (2003).
[3] S. M. Ponder, J. C. Darab, T. E. Malouk, Environ. Sci. Technol., **34**, 2564 (2000).
[4] R. Quiao, C. Yang, M. Gao, J. Mater. Chem., **19**, 6274 (2009).
[5] Y. Zhang, S. W. Y. Gong, L. Jin, S. M. Li, Z. P. Chen, M. Ma, N. Gu, Chin. Chem. Lett., **20**, 969 (2009).
[6] S. Kayal, R. V. Ramanujan, Mater. Sci. Eng. C, **30**, 484 (2010).
[7] M. Levy1, C. Wilhelm, J.-M. Siaugue, O. Horner, J.-C. Bacri, F. Gazeau, J. Phys. Condens. Matter ., **20**, 204133 (2008).
[8] A. Amir, W. Lee, J. Hazard.Mater., **235– 236**, 359 (2012).
[9] J. Bagheriyan, J. Chem. Chem. Eng., **9**, 824 (2011).
[10] D. Fan, R. P. Anitori, B. M. Tebo, P. G. Tratnyek, J. S. L. Pacheco , R. K. Kukkadapu, M. H. Engelhard, M. E. Bowden, L. Kovarik, B. W. Arey, Environ. Sci. Technol., **47**(10), 5302 (2013).
[11] J. Puthussery, S. Seefeld, N. Berry, M. Gibbs, M. Law, J. Am. Chem. Soc., **133**, 716 (2011).
[12] B. Wu, H. Song, J. Zhou, X. Chen, Chem. Commun., **47**, 8653 (2011).
[13] F.-L. Pua, C.-H. Chia, S. Zakaria, S.-K. Neoh, T.-K. Liew, Sains Malaysiana, **40**(3), 221 (2011).
[14] J. M. Stencel, P. C. Eklund, X.-X. Bi, B. H. Davis, G. T. Hager, F. J. Derbyshire, Stud. Surf. Sci. Catal., **75**(2), 1797 (1993).
[15] X.-X. Bin, B. Ganguly, G. P. Huffman, M. Endo. P. C. Eklund, J. Mater. Res., **8**(7), 1666 (1993).
[16] S. Veintemillas-Vendaguer, M. P. Morales, C. J. Serna, Mater Lett., **35**, 227 (1998).
[17] F. Dumitrache, I. Morjan, C. Fleaca, R. Birjega, E. Vasile, V. Kuncser, R. Alexandrescu, Appl. Surf. Sci. **257**, 5265 (2011).
[18] C. T. Fleaca, F. Dumitrache, I. Morjan, R. Alexandrescu, I. Sandu, C. Luculescu, S. Birjega, G. Prodan, I. Stamatin, Appl. Surf. Sci., **258**, 9394 (2012).
[19] J. Pola, Z. Bastl, V. Vorlicek, F. Dumitrache, R. Alexandrescu, I. Morjan, I. Sandu, V. Ciupina, Appl. Organomet. Chem. **18**, 337 (2004).
[20] F. Dumitrache, I. Morjan, R. Alexandrescu, R. E. Morjan, I. Voicu, I. Sandu, I. Soare, M. Ploscaru, C. Fleaca, V. Ciupina, G. Prodan, B. Rand, R. Brydson , A. Woodword, Diamond. Relat. Mater., **13**, 362 (2004).
[21] J. D. van Drumpt, Rev. Trav. Chim. Pays-Bas, **91**(8), 906 (1972).
[22] G. A Razuraev, V. S. Eltis, L. N. Grobov, Zh. Obshch. Khim., **33**, 1366 (1963).
[23] R. D. Adams, N. M. Golembeski, J. P. Selegue, J. Am. Chem. Soc., **103**(3), 546 (1981).
[24] F. Dumitrache, I. Morjan, R. Alexandrescu , V. Ciupina, G. Prodan, I. Voicu, C. Fleaca, L. Albu, M. Savoiu, I. Sandu, E. Popovici, I. Soare, Appl. Surf. Sci., **247**, 25 (2005).
[25] C. T. Fleaca, I. Morjan, R. Alexandrescu, F. Dumitrache, I. Soare, L. Gavrila-Florescu, F. Le Normand, W. Derory, Appl. Surf. Sci., **255**, 5386 (2009).

*Corresponding author: claudiufleaca@yahoo.com